

77135**Vesicular Poikilitic Impact Melt Rock
337.4 g, 10.3 x 8.0 x 4.0 cm****INTRODUCTION**

Sample 77135 was sampled as "green-grey breccia" from the boulder at Station 7 (*see the section on the Station 7 Boulder, page 235*). It is similar in texture and composition to 76015 and other rocks from the boulders on the North Massif (Chao et al., 1975, and Winzer et al., 1975). The probable origin of impact melt breccias has been explained by Simonds (1975) and Onorato et al. (1976). However, members of the international consortium were impressed with arguments that this rock may have an igneous origin (see for example Chao and Minkin, 1974).

Sample 77135 is a vesicular, grey, fragment-laden, fine-grained, crystalline-matrix breccia (Minkin et al., 1978). It has two parts: a larger, highly vesicular part and a smaller, less vesicular, finer-grained part (Figs. 1-3). The highly vesicular part includes clasts of recrystallized troctolitic anorthosite. Major clasts present in the less vesicular part include recrystallized troctolitic breccia. 77135 is stratigraphically the youngest lithology on the Station 7 Boulder, and this seems to be confirmed by age dating.

PETROGRAPHY

Chao et al. (1974), Bence et al. (1974), Chao and Minkin (1975), and McGee et al. (1980) have provided descriptions of 77135. Sample 77135 contains two textually distinct fragment-laden melt rock units (seen in Fig. 3): a coarser-grained matrix fraction that contains vesicles 100-500 μm in diameter and a finer-grained matrix fraction that contains 50-150 μm vesicles. Bence et al. (1974) describe the texture as poikiloblastic, while members of the international consortium (Minkin et al., 1978) refer to it as "fragment-



Figure 1: Photograph of 77135, illustrating vesicles and clasts. Cube is 1 cm. S72-56391.



Figure 2: Photograph of a piece of 77135 showing dark patina. Cube is 1 cm. S72-56387.

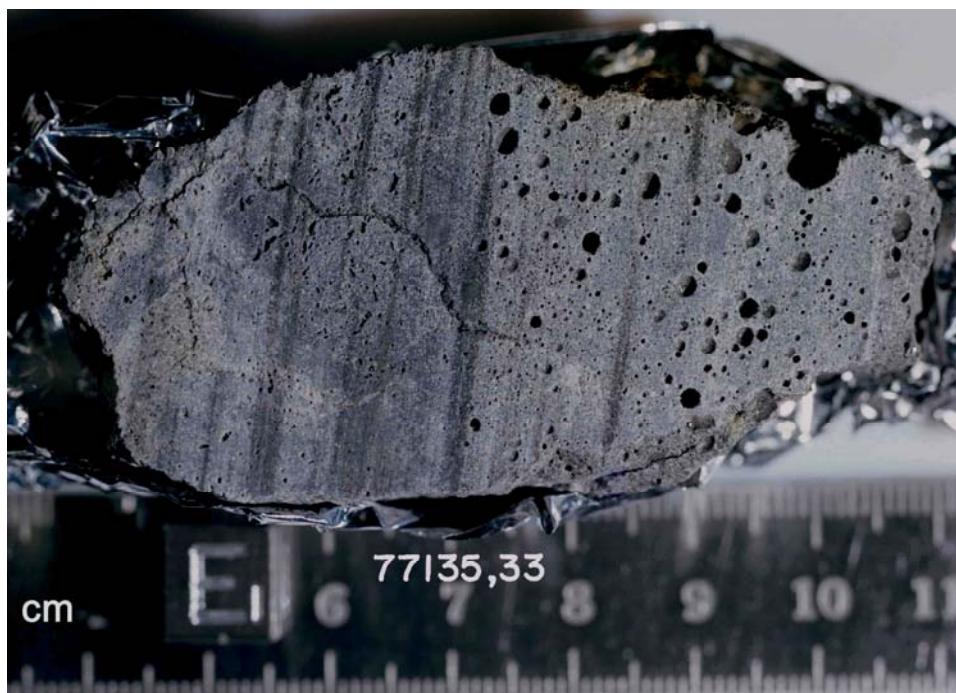


Figure 3: Photograph of slab surface of 77135. S73-34469.

laden, pigeonite basalt." Mineral fragments, mostly plagioclase and olivine, are more abundant in the coarser fraction. The matrix of the coarser fraction consists predominantly of poikilitic pyroxene (mostly pigeonite with minor augite) enclosing subhedral to euhedral plagioclase (Fig. 4). Borders between the pyroxene oikocrysts contain granular olivine, ilmenite plates and rods, and mesostasis. The pyroxene oikocrysts generally are 200-600 μm in size, but some oikocrysts are larger than 1 mm. The finer fraction commonly surrounds or is adjacent to large lithic clasts. The matrix of the finer fraction also consists predominantly of poikilitic pyroxenes (75-200 μm) enclosing plagioclase. Plagioclase grains are finer and more irregular than in the coarser fraction. Intergrowths of rounded, small (<20 μm) olivine grains and irregular plagioclase grains form aggregates of approximately the same size as the pyroxene oikocrysts. Plates and rods of ilmenite mark the borders between the oikocrysts and olivine-plagioclase intergrowths.

Chao and Minkin (1975) calculate the CIPW norm as 53% plagioclase, 31% pyroxene, 13% olivine, and 3% ilmenite. Vaniman and Papike (1979) give the mode of the matrix as 41.1% plagioclase, 30% pyroxene, 15% olivine, and 1.4% ilmenite (with 6.2% plagioclase and 2% pyroxene clasts). Plagioclase in the matrix occurs in two distinct morphological types: as small, sharply defined laths or elongated platy inclusions (An_{91}) in the poikilitic pyroxene, and as stubby laths and anhedral grains associated with granular olivine grains (An_{89}). The dominant pyroxene in the matrix is pigeonite ($\text{Wo}_{5-12}\text{En}_{67-76}\text{Fs}_{19-21}$). Augite is minor. The olivine occurs both as rounded inclusions in the pigeonite (Fo_{66-79}) and as irregular grains associated with the anhedral plagioclase (Fo_{64-72}).

The poikilitic texture of 77135 is the result of enhanced growth of pyroxene and ilmenite enclosing smaller grains of feldspar and olivine. Olivine may also enclose feldspar laths. Simonds et al. (1973) suggest that poikilitic texture is a

result of two-stage cooling: initial rapid cooling near the coetectic with nucleation of feldspar and olivine at many foci, followed by slower cooling and crystallization at the point where pyroxene saturation is reached, allowing the growth of large pyroxene grains encompassing the previous crystals. Ryder and Bower (1976) and Lofgren (1977) suggest that nucleation effects (e.g., many nucleation sites) are important in the origin of this texture.

Storey et al. (1974) and Ford (1976) have studied 77135 experimentally. Storey et al. have concluded that 77135 would not be a liquid at less than 1280 $^{\circ}\text{C}$, 1 atmosphere pressure.

Note: This sample was chosen as part of the "suite" of reference samples for the Basaltic Volcanism Study. It was considered a "highland" basalt even though it had a texture of an impact melt! Its apparent importance is that its composition is very near the coetectic of the low-pressure phase diagram of Walker et al. (1973).

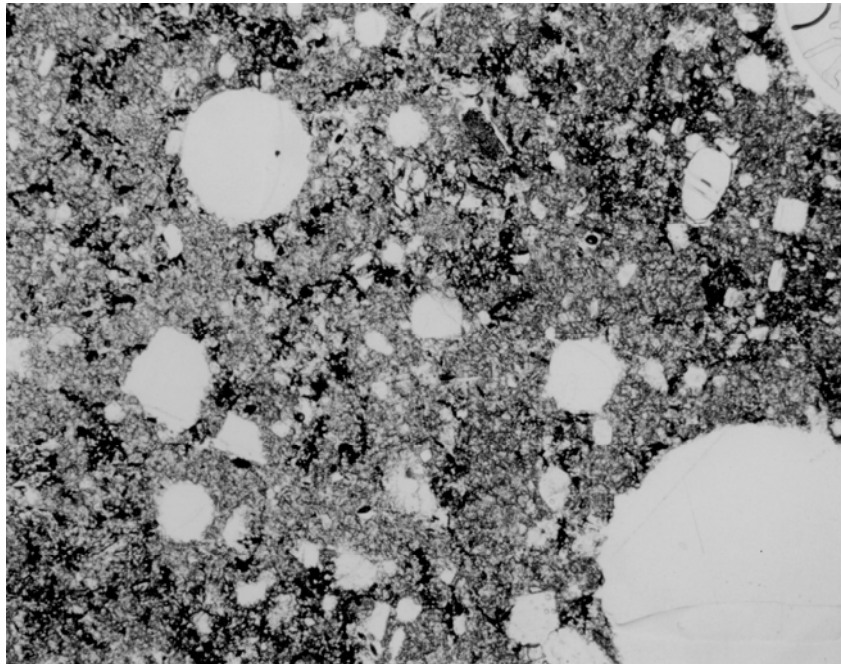


Figure 4: Photomicrograph of 77.135,7, showing vesicles and the micropoikilitic texture of the matrix. Field of view is 3 x 5 mm.

MINERAL CHEMISTRY

The composition of minerals in 77135 is given in Bence et al. (1974), Chao and Minkin (1974), Vaniman and Papike (1980), and McGee et al. (1980) (Figs. 5 and 6). McGee et al. have studied the microstructures in the pyroxenes from the different lithologies of the Station 7 Boulder, including 77135. Steele et al. (1980) have analyzed the plagioclase by ion probe. Smith et al. (1980) and Ryder (1992) have analyzed olivine, and Engelhardt (1979) has studied the ilmenite in 77135. Hewins and Goldstein (1975) report Ni-rich metal grains in a clast in 77135.

WHOLE-ROCK CHEMISTRY

Winzer et al. (1974 and 1977), Rhodes et al. (1974), and Hubbard et al. (1974) have analyzed 77135 (Tables 1 and 2 and Fig. 7). Higuchi and Morgan (1975) and Morgan et al. (1974) have measured the trace siderophile and volatile element contents of 77135 (Table 3). None of the clasts was found to have: low Ir.

Gibson and Moore (1974) report sulfur abundances, and Gibson et al. (1987) reported the hydrogen content.

SIGNIFICANT CLASTS

Winzer et al. (1974) present trace element data (Table 2, Fig. 7) for two pronounced clasts in 77135 ("troctolite" clast 77135,52 and "olivine-rich" clast 77135,57). The numbering and original distribution of splits of these two clasts are given in Butler and Dealing (1974). Chao et al. (1974) give petrographic descriptions and mineral analyses of these xenoliths. Minkin et al. (1978) also discuss the clast types in 77135, but it is sometimes difficult to tell which data are from which clast.

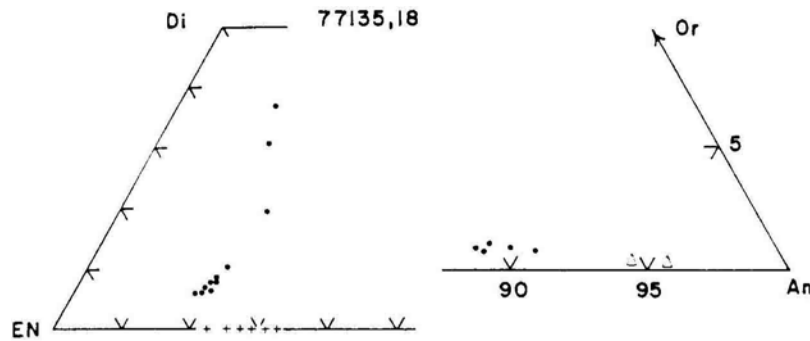


Figure 5: Pyroxene diagram for the matrix of 77135. From Bence et al. (1974).

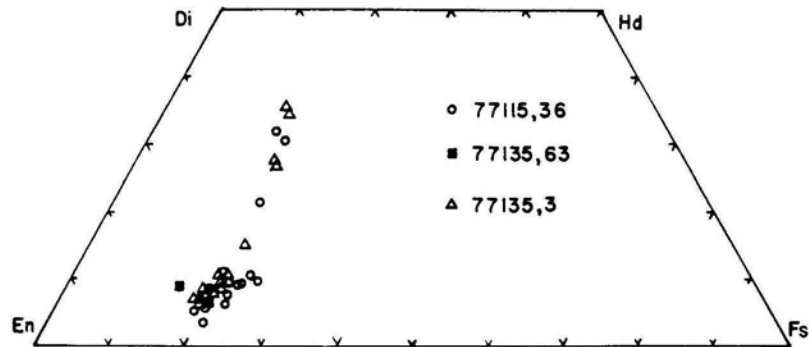


Figure 6: Pyroxene diagram for 77135 compared with 77115. From McGee et al. (1980).

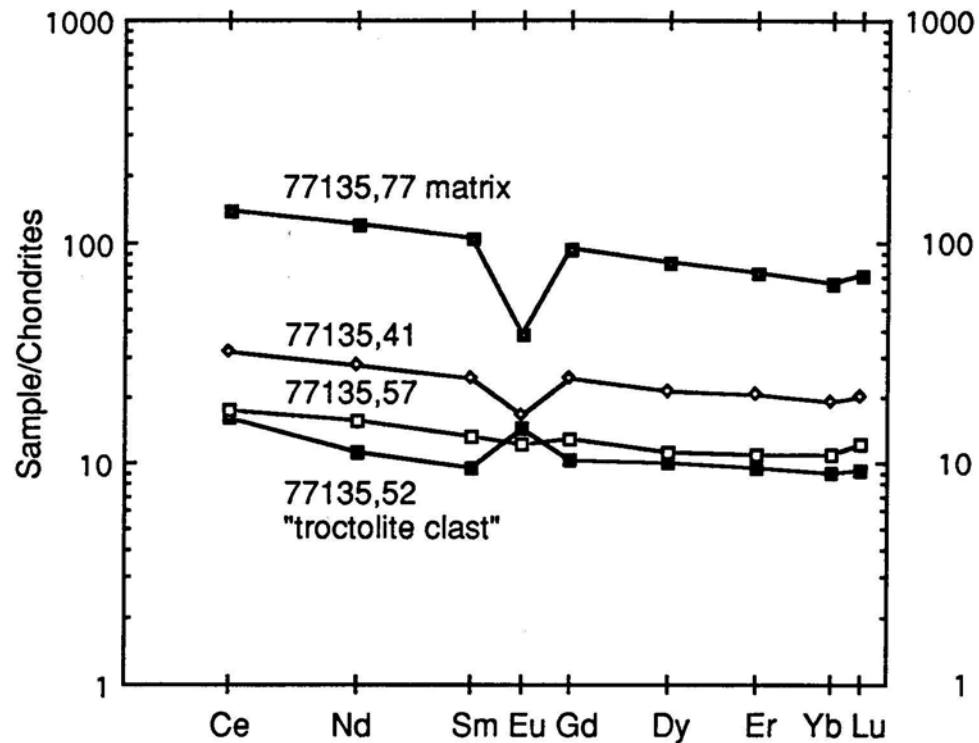


Figure 7: Normalized rare earth element diagram for the matrix and selected clasts in 77135. Data from Winzer et al. (1977) and Hubbard et al. (1974).

Clast 1 (the "olivine-rich" cast ,57) was found to have very high Ir by Higuchi et al. (1975). Nunes et al. (1974) determined a Rb-Sr internal isochron of 3.89 ± 0.08 b.y. for cast 1 (Fig. 8) and Stettler et al. (1978) dated cast 1 at 3.88 ± 0.05 b.y. (Fig. 9) by the Ar-Ar plateau technique.

Clast 2 (the "troctolite" clast ,52) was also studied by Morgan et al. (1974), who again found high In Stettler et al. (1974) dated a split (,51) of this clast at 3.99 ± 0.02 b.y. (Fig. 10).

RADIOGENIC ISOTOPES

Turner and Cadogan (1975) found that 77135 gave a very poor Ar release pattern, preventing an accurate age determination. Stettler et al. (1974) determined ^{39}Ar - ^{40}Ar ages of 3.83 ± 0.04 b.y. and $3.78 \pm$

0.08 b.y. for the vesicular matrix and 3.99 ± 0.02 b.y. and 4.00 ± 0.03 b.y. for the troctolitic cast in 77135 (Figs. 9, 10, and 11). Stettler et al. (1975) report an age of 3.90 ± 0.03 Ky. for a matrix sample and an olivine-rich clast (,57). Stettler et al. (1978) determined ages of 3.88 ± 0.05 b.y. and 3.87 ± 0.04 b.y. for the recrystallized clast 1 (Fig. 9) and concluded that the cooling age of the green-grey breccia was 3.89 ± 0.04 b.y. This is the same age as determined for 77115 by the same laboratory.

Nunes et al. (1974) report a Rb-Sr internal isochron age of 3.89 ± 0.08 b.y. for class 1 (,57) of 77135 (Fig. 8). Nyquist et al. (1974) report Rb-Sr data for the matrix of 77135 (Table 4) and note that the Rb-Sr systematics for "noritic breccias" at Apollo 17 are probably partially reset by the Serenitatus impact event (Fig. 12). Nakamura et al. (1976)

determined an apparent age of 4.14 ± 0.08 b.y. (Fig. 13), but they surmisi; that this "isochron" is a mixing line between partially reset old plagioclase xenoliths and the young matrix (Table 5). In this case, no age significance should be given to this mixing line.

Nunes et al. (1974) report U-Th-Pb data for 77135 (Table 6).

COSMOGENIC RADIOISOTOPES AND EXPOSURE AGES

Turner and Cadogan (1975) determined an exposure age of 23 m.y., Crozaz et al. (1974) determined an age of 28.6 m.y., and Stettler et al. (1974) determined an age of 28.5 and 29.6 m.y. Eberhardt et al. (1975) determined 31.8 ± 1.6 m.y. by ^{81}Kr -Kr and 20 ± 2 m.y. by ^{37}Ar -Ar. The Ar exposure age is sensitive to

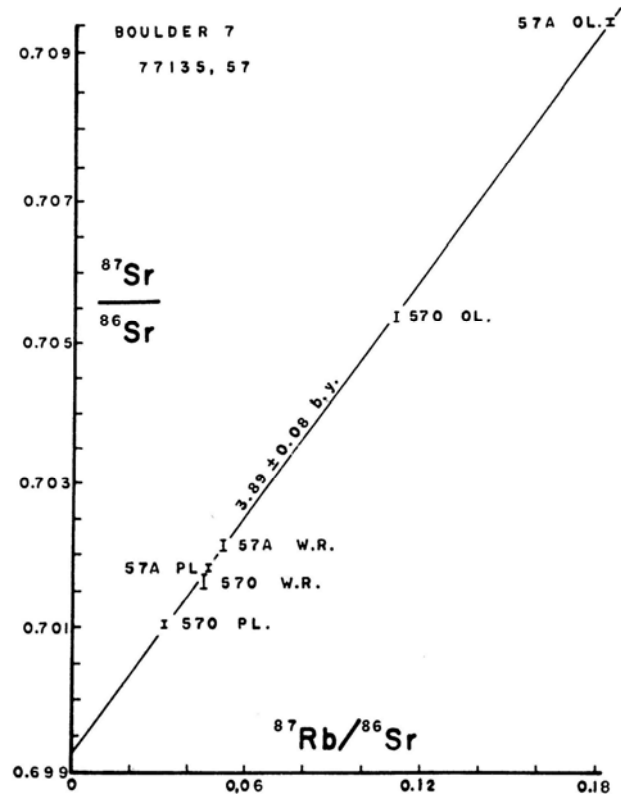


Figure 8: Rb-Sr internal isochron of an olivine-rich clast (57) in 77135. From Nunes et al. (1974).

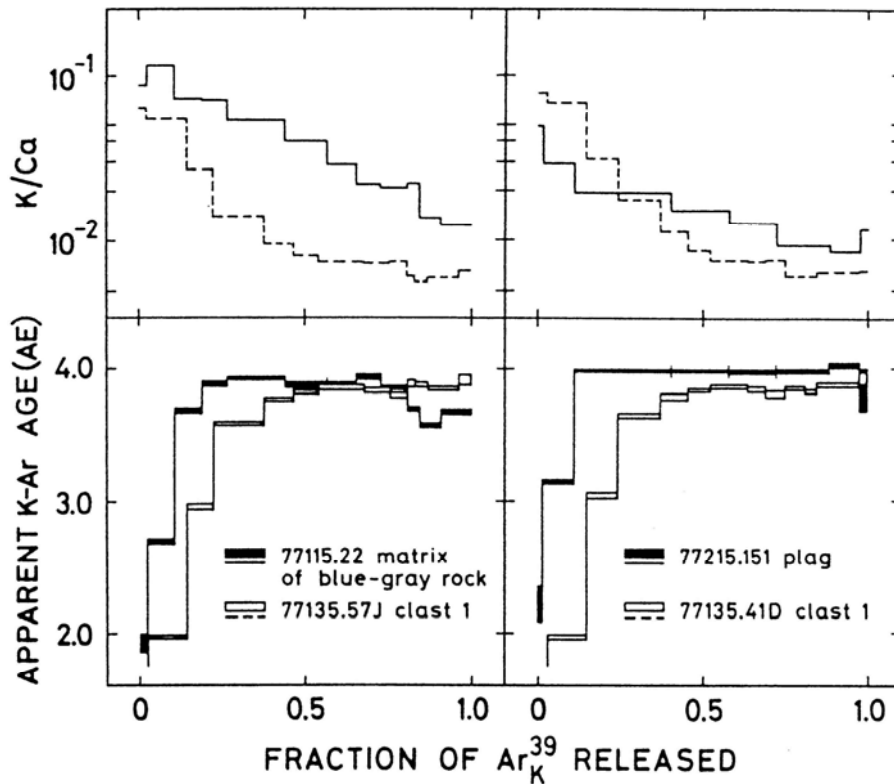


Figure 9: ^{39}Ar ^{40}Ar temperature release pattern for 77135 clast 1 (57). From Stettler et al. (1978).

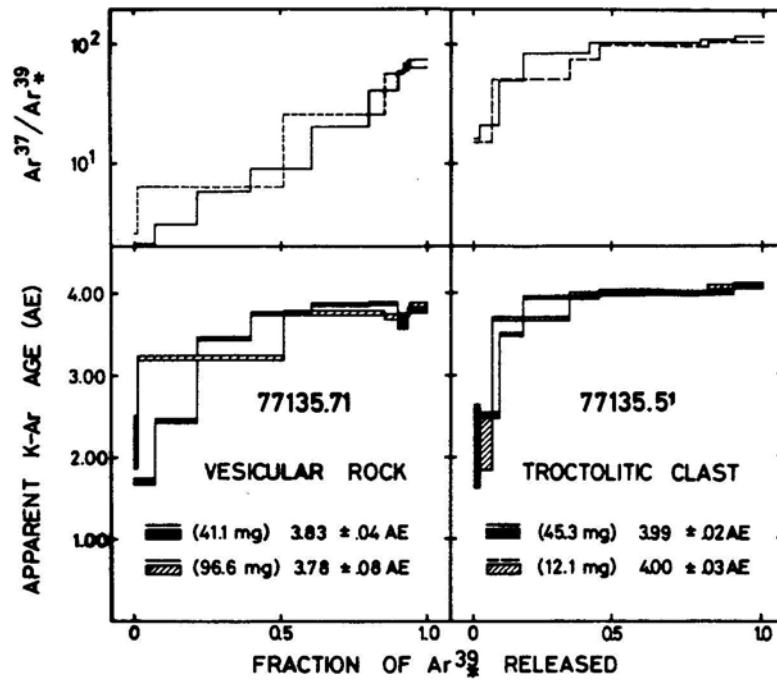


Figure 10: ^{39}Ar - ^{40}Ar temperature release patterns for 77135 clast 2 (.51) and vesicular matrix. From Stettler et al. (1974).

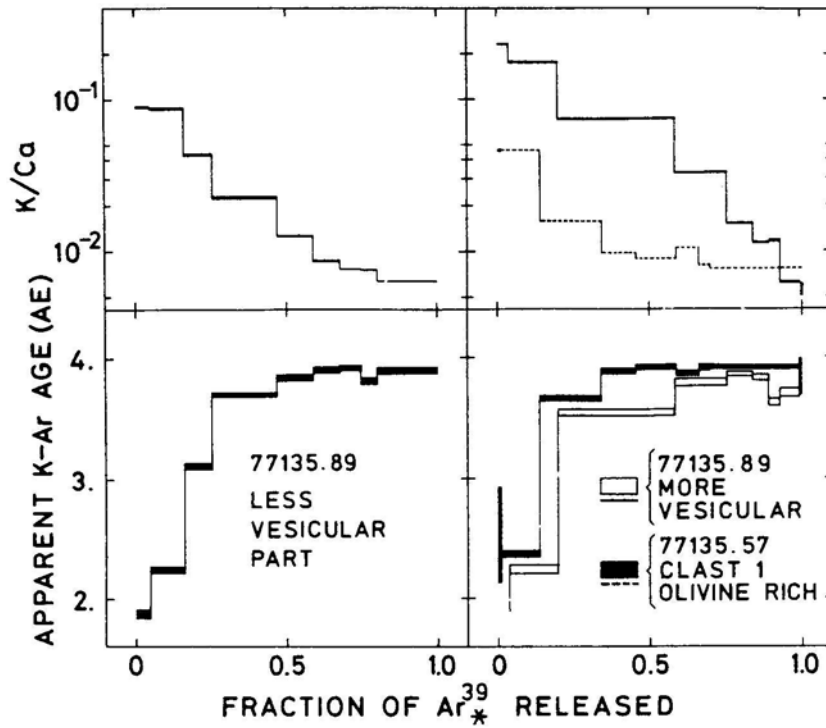


Figure 11: ^{39}Ar - ^{40}Ar temperature release patterns for 77135 vesicular matrix. From Stettler et al. (1975).

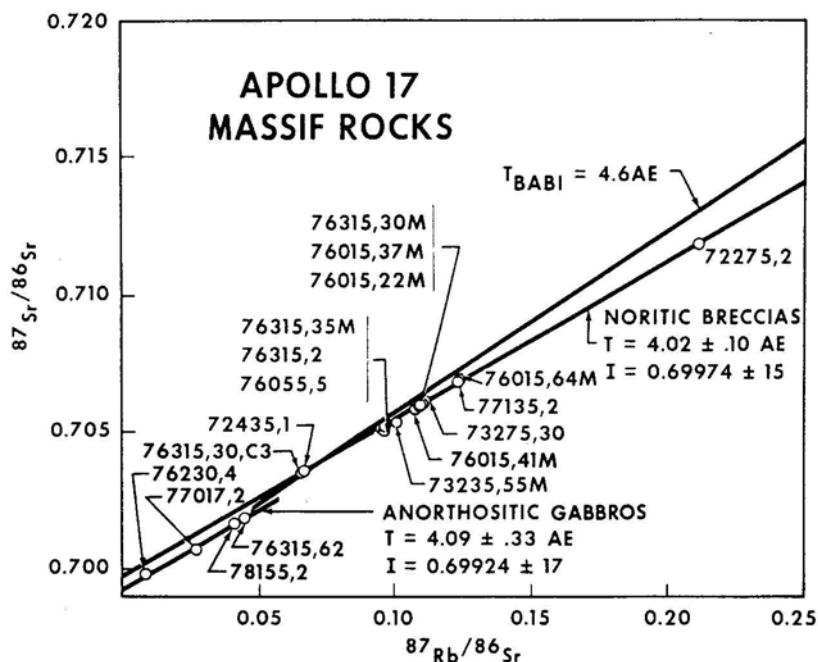


Figure 12: Whole-rock isochron for noritic breccias from Apollo 17, including 77135. From Nyquist et al. (1974).

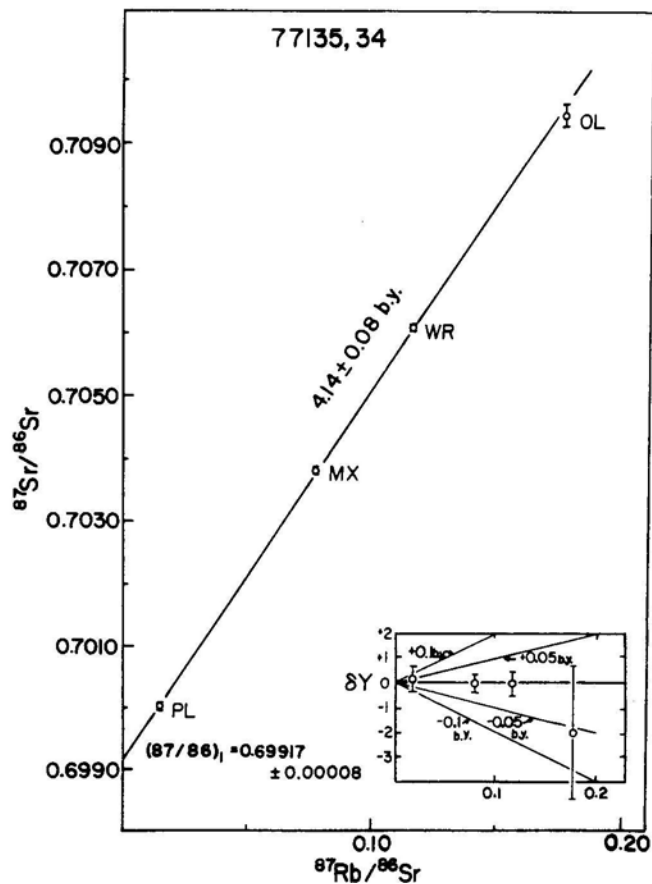


Figure 13: Apparent Rb-Sr internal "isochron," or mixing line, for the 77135 matrix, including small plagioclase xenoliths. No significance should be given to this "age" (see discussion). Figure from Nakamura et al. (1976).

shielding by part of the boulder, whereas the Kr exposure age is not. Eugster et al. (1984) have also discussed the exposure age of 77135.

Some of the Apollo 17 samples (including 77135) provided a unique opportunity to study the energy spectrum (and potential angular anisotropy) of the incident proton flux from the August 1972 solar flare (Rancitelli et al., 1974; Keith et al., 1974). Table 7 compares the induced activity of 77135 with other samples of Apollo 17 (see also table for 76215). Yokoyama et al. (1974) discussed the cosmogenic isotopes.

MAGNETIC STUDIES

771.35 has been used for numerous studies of the magnetic properties of an old, well-dated lunar rock. Cisowski et al. (1983) have determined the thermal remanent magnetization of 77135. Nagata (1975) has reported the intensity of saturation magnetization for 77135. Pierce et al. (1974) and Brecher (1975) have studied the direction of magnetization, and Brecher (1977) has discussed apparent alignment with petrofabric. Hale et al. (1978) have used microwave heating to improve demagnetization experiments (Fig. 15).

Brecher (1975) has determined the Massbauer spectra of 77135 (Fig. 14).

SURFACE STUDIES

Adams and Charette (1975) have determined the spectral reflectance of 77135 (Fig. 16). Fechtig et al. (1974) have studied the microcraters on the surface of 77135.

PROCESSING

The initial processing and distribution of 77135 is outlined in Butler and Dealing (1974). It was studied by the international consortium led by E.C.T. Chao (Minkin et al., 1978). Detailed description of the splits is given in open-file report 78-511.

The largest remaining piece of 77135 weighs 234 g. There have been 34 thin sections prepared.

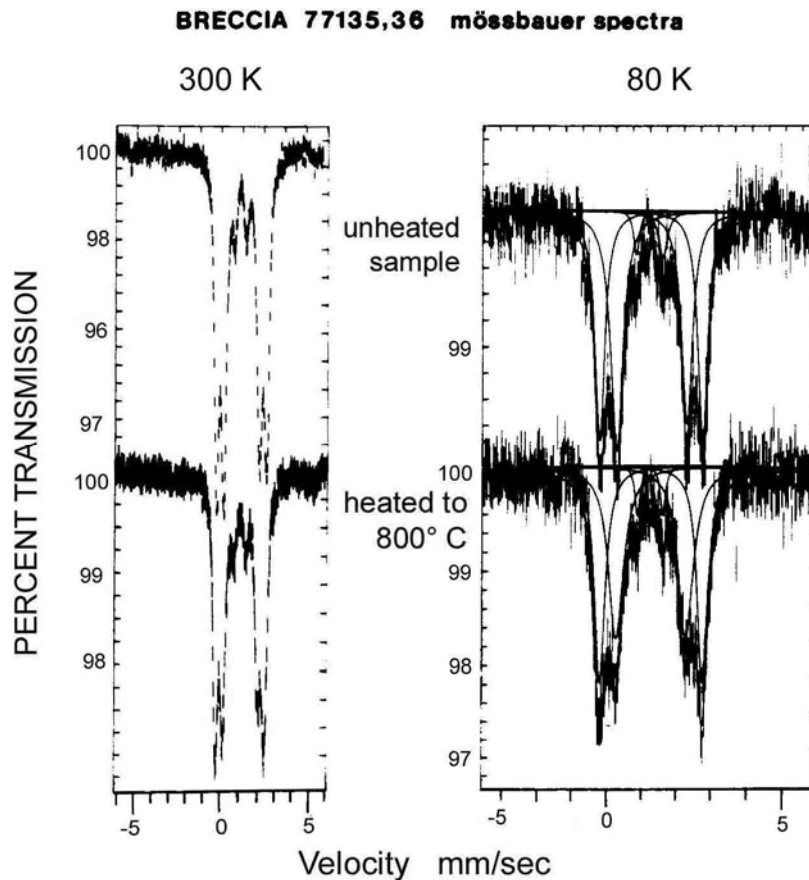


Figure 14: Mossrhauer spectra for 77135. From Brecher (1975).

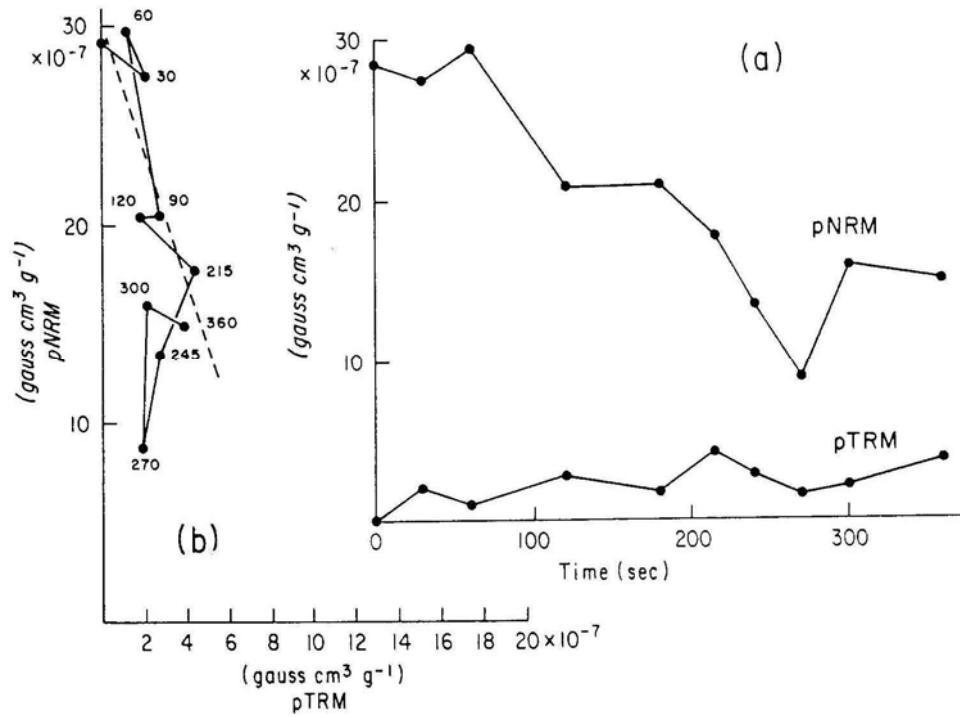


Figure 15: Demagnetization curve for 77135. From Hale et al. (1978).

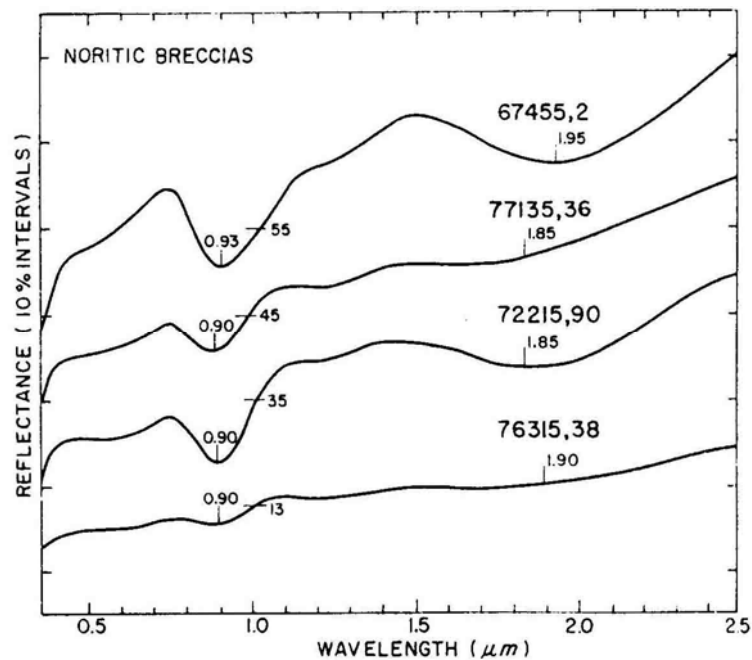


Figure 16: Spectral reflectance of 77135. From Adams and Charette (1975).

Table 1: Whole-rock chemistry of 77135.

a) Rhodes et al. (1974); b) LSPET (1973); c) Hubbard et al. (1974);
 d) Wiesmann and Hubbard (1975); e) Winzer et al. (1977)

Split Technique	,2 (b, c, d) XRF, ID	,5 (a) XRF	,82 (e) AA, IDMS matrix	,92 (e) AA, IDMS matrix
SiO ₂ (wt%)	46.13	46.17	47.5	46.3
TiO ₂	1.54	1.53	1.45	1.31
Al ₂ O ₃	18.01	17.83	17.18	19.82
Cr ₂ O ₃	0.20	0.21	0.18	0.16
FeO	9.11	9.14	9.01	8.28
MnO	0.13	0.13	0.11	0.10
MgO	12.63	12.39	12.66	11.78
CaO	11.03	11.08	10.91	11.74
Na ₂ O	0.53	0.69	0.66	0.56
K ₂ O	0.30	0.27	0.41	0.21
P ₂ O ₅	0.28	0.30	0.29	0.21
S	0.08	0.07		
Nb (ppm)	33	33		
Zr	494	508		
U	1.50			
Th	5.60			
Y	107	111		
Sr	172	174	177	171
Rb	7.32	6.2		
Li	19.3			
Ba	337		360	294
Zn	4	4		
Ni	110	62		
La	32.1			
Ce	81.2		82.8	59.2
Nd	51.6		53.2	41.1
Sm	14.6		14.8	11.2
Eu	1.99		1.97	1.80
Gd	18.5			
Dy	19.1		18.3	15.1
Er	11.4		(1.4)	8.16
Yb	10.5		10.6	8.11
Lu	1.55		1.18	1.17

Table 2: Whole-rock and clast chemistry of 77135.

a) Winzer et al. (1974); b) Winz.-r et al. (1977)

Split Technique	,66 (a) AA, IDMS matrix	,77 (a) AA, IDMS matrix	,41 (a) AA, IDMS Ol-Pl breccia	,52 (a, b) AA, IDMS Troctolite	,57 (a) AA, IDMS Ol-rich
SiO ₂ (wt%)	45.3	46.3	45.3	44.4	
TiO ₂	1.72	1.48	0.43	0.24	
Al ₂ O ₃	18.03	18.39	25.13	27.81	
Cr ₂ O ₃	0.18	0.18	0.13	0.09	
FeO	9.56	9.48	5.98	4.19	
MnO	0.11	0.11	0.06	0.05	
MgO	13.38	12.19	8.59	7.96	
CaO	10.64	10.96	13.95	15.09	
Na ₂ O	0.61	0.65	0.40	0.41	
K ₂ O	0.22	0.23	0.09	0.07	
P ₂ O ₅	0.28	0.28	0.10	0.03	
Nb (ppm)					
Zr	308	643	146	62.1	71.8
Sr	169	181	147	147	87.4
Rb	5.99	6.63	2.67	2.00	1.18
Li	18.4	19	10.2	10.1	10.6
Ba	343	359	96.6	63.3	60.8
La					
Ce	81.2	83.3	19.4	9.63	10.5
Nd	52.2	54.6	12.7	4.99	7.14
Sm	14.7	15.4	3.62	1.41	1.96
Eu	2.02	2.16	0.919	0.80	0.687
Gd	18.6	18.6	4.73	2.03	2.51
Dy	19.3	20.0	5.07	–	2.69
Er	11.4	11.6	3.24	1.50	–
Yb	–	10.6	3.08	1.45	1.79
Lu	1.56	1.75	0.481	0.223	0.293

Table 3: Trace element data for 77135. Concentrations in ppb.
 From Morgan et al. (1974x) and Higuchi and Morgan (1975a).

	Sample 77135,10	Sample 77135,50	Sample 77135,62	Sample 77135,57	Sample 77135,69
Ir	3.78	7.2	15.1	17.4	10.5
Os					
Re	0.485	0.662	1.42	1.38	1.06
Au	3.57	1.46	4.74	3.09	6.45
Pd					
Ni (ppm)	205	174	412	221	438
Sb	1.21	0.58	0.47	0.778	2.16
Ge	295	50	78	113	618
Se	137	11.3	33	40	144
Te	3.6	1.32	1.1	5	8.84
Ag	1.1	0.38	0.58	0.7	1.2
Br	47	11.6	17.6	35.7	45
In					
Bi	0.18	0.17	0.14	0.25	0.23
Zn (ppm)	2.9	2.6	2.4	2	3.3
Cd	10.5	6.8	3.7	2.4	3.5
Tl	2.6	0.48	0.58	0.8	2.3
Rb (ppm)	6.5	1.8	2.6	3.59	6.1
Cs	270	74	73	95.3	250
U	1390	260	450	590	1380

Table 4: Rb-Sr composition of 77135.

Data from Nyquist et al. (1974).

Sample	77135,2
wt (mg)	52.6
Rb (ppm)	7.32
Sr (ppm)	172.2
$^{87}\text{Rb}/^{86}\text{Sr}$	0.1230 ± 10
$^{87}\text{Sr}/^{86}\text{Sr}$	0.70688 ± 7
T _B	4.41 ± 0.08
T _L	4.45 ± 0.08

B = Model age assuming $I = 0.69910$ (BABI + JSC bias)

L = Model age assuming $I = 0.69903$ (Apollo 16 anorthosites for $T = 4.6$ b.y.)

Table 5: Rb-Sr composition of 77135,34.

Data from Nakamura et al. (1976).

Separate	Plag.	Olivine	Whole Rock	Matrix
wt (mg)	4.94	6.36	7.23	5.35
K (%)	0.056	0.028	0.226	0.116
Rb (ppm)	0.911	0.818	6.77	3.77
Sr (ppm)	157.4	13.27	167.5	140.2
$^{87}\text{Rb}/^{86}\text{Sr}$	0.01547	0.1766	0.1168	0.0777
$^{87}\text{Sr}/^{86}\text{Sr}$	0.70007 ± 4	0.70943 ± 19	0.70608 ± 3	0.70381 ± 3

Table 6: U-Th-Pb for 77135.

From Nunes et al. (1974).

Split	77135,33	,34	,57A
wt (mg)	133.2	125	122.1
U (ppm)	0.4674	1.390	0.5461
Th (ppm)	1.863	5.224	2.136
Pb (ppm)	0.9713	2.840	1.115
$^{232}\text{Th}/^{238}\text{U}$	4.12	3.88	4.04
$^{238}\text{U}/^{204}\text{Pb}$	1387	2755	1191

Table 7: Solar flare induced activity from large solar flare, August 1972.

a) Rancitelli et al. (1974); b) Keith et al. (1974); c) O'Kelley et al. (1974)

	Sample 77135 (a)	Sample 78135 (b)	Sample 78235 (b)	Sample 78255 (b)	Sample 78597 (c)
dpm/Kg					
²⁶ Al	111 ± 6	42 ± 4	77 ± 7	65 ± 6	48 ± 4
²² Na	100 ± 5	74 ± 5	111 ± 8	50 ± 5	33 ± 4
⁵⁴ Mn	21 ± 15	180 ± 20	55 ± 8	10 ± 5	80 ± 10
⁵⁶ Co	66 ± 4	240 ± 20	52 ± 9	30 ± 20	80 ± 20
⁴⁶ Sc	7.2 ± 2.2	76 ± 5	1.4 ± .9	<15	25 ± 10
⁴⁸ V		18 ± 5	<12		
Th (ppm)	5.51	.26	.59	.83	
U (ppm)	1.42	.107	.196	.227	
K (%)		.0525	.049	.059	